Discovery of Novel 15-Lipoxygenase Activators To Shift the Human Arachidonic Acid Metabolic Network toward Inflammation Resolution

Hu Meng,[†] Christopher L. McClendon,[∥] Ziwei Dai,[‡] Kenan Li,[§] Xiaoling Zhang,[‡] Shan He,[†] Erchang Shang,[†] Ying Liu,[†,‡] and Luhua Lai*,[†,‡,§]

[†]BNLMS, State Key Laboratory for Structural Chemistry of Unstable and Stable Species, College of Chemistry and Molecular Engineering, [‡]Center for Quantitative Biology, and [§]Peking−Tsinghua Center for Life Sciences, Peking University, Beijing 100871, China

[∥]Skaggs School of Pharmacy and Pharmaceutical Sciences, University of California San Diego, La Jolla, California 92093, United States

S *Supporting Information*

ABSTRACT: For disease network intervention, up-regulating enzyme activities is equally as important as down-regulating activities. However, the design of enzyme activators presents a challenging route for drug discovery. Previous studies have suggested that activating 15-lipoxygenase (15-LOX) is a promising strategy to intervene the arachidonic acid (AA) metabolite network and control inflammation. To prove this concept, we used a computational approach to discover a previously unknown allosteric site on 15-LOX. Both allosteric inhibitors and novel activators were discovered using this site. The influence of activating 15-LOX on the AA metabolite network was then investigated experimentally. The activator was found to increase levels of 15-LOX products and reduce production of pro-inflammatory mediators in human whole blood assays. These results demonstrate the promising therapeutic value of enzyme activators and aid in further development of activators of other proteins.
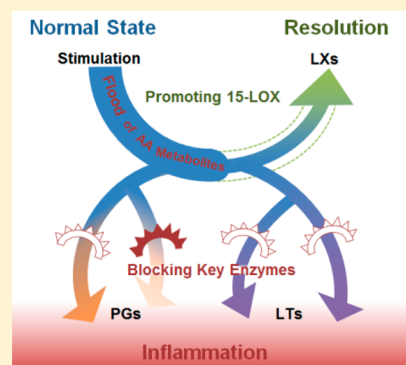
INTRODUCTION

The majority of current chemical biology and drug discovery approaches to regulate target activity focus on the development of small-molecule inhibitors. However, there are also significant advantages to developing enzyme activators.[1] In human cells, arachidonic acid (AA) is metabolized into a large family of pro-inflammatory eicosanoids, including leukotrienes (LTs) and prostaglandins (PGs), through two major pathways involving 5-lipoxygenase (5-LOX) and cyclooxygenase (COX)[2] (Figure 1). Most studies of anti-inflammatory drugs focus on discovering inhibitors that target key enzymes in the 5-LOX and COX pathways.[2] However, previous studies[3−5] have suggested that inhibiting one of these enzymatic pathways shifts the metabolism of AA toward the other pathway, which may cause adverse effects. In the 1980s, Serhan et al. discovered a series of oxygenated derivatives formed from AA in human leukocytes called lipoxins (LXs),[6] which demonstrated anti-inflammatory activity as well as the capacity to promote the resolution of inflammation and return to tissue homeostasis. Utilizing the effects of these pro-resolving molecules would activate the body's natural pathways for curbing inflammation and should be safer than current anti-inflammation therapeutic strategies.[7] However, LXs are difficult to synthesize and unstable, which prevents further usage of these compounds for inflammation control.
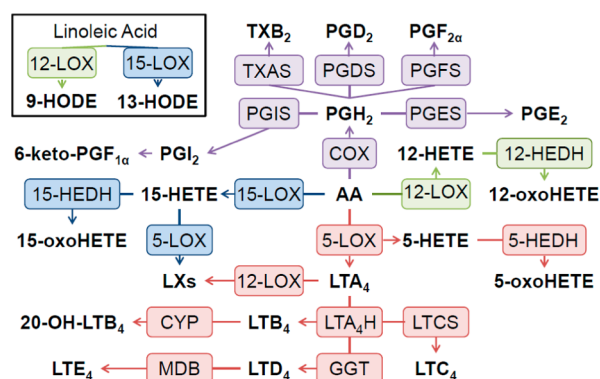

Figure 1. Major eicosanoid biosynthesis pathways in the AA metabolic network. Red, 5-LOX pathway; purple, COX pathway; green, 12-LOX pathway; blue, 15-LOX pathway.

Human reticulocyte 15-lipoxygenase (15-LOX type 1, 15-LOX-1) is one of the key enzymes involved in the generation of LXs.[8] Besides LXs, products of 15-LOX-1, including 15-

hydroxyecosatetraenoic acid (15-HETE) and 13-hydroxy-octadecadienoic acid (13-HODE), also exhibit anti-inflammatory activities.[9−11] Moreover, previous studies of the topology and dynamic properties of the AA metabolic network in computational models[3,12] demonstrated that activation of 15-LOX-1 reduces the formation of LTs and PGs. These facts imply that 15-LOX-1 can be activated for therapeutic benefit. However, the effects of activating specific nodes in the AA network have not been evaluated due to a lack of proper methods for identifying enzyme activators.

However, discovering activators is much more challenging than identifying inhibitors. The design of activators requires information about allosteric sites and knowledge of the mechanism of activation, both of which are rarely available for most enzymatic targets. Therefore, rational approaches for discovering activators have been applied to only a limited number of targets.[13,14] Experimental high-throughput screening is the most commonly used method for identifying activators.[15−17] However, this method generally requires significant effort and is often serendipitous. In the present study, we proposed a rational strategy to discover allosteric activators of 15-LOX-1 (referred to as 15-LOX below), for which information about allosteric sites and structural details of the activated state remain unknown.[18,19] We searched for possible allosteric sites using the mutual information method (MutInf[20]) in combination with a method that identifies pockets and predicts their druggability (CAVITY).[21,22] A virtual screening was conducted against the predicted allosteric sites, and novel activators and inhibitors were discovered. Using the most potent 15-LOX activator as a molecular probe, we studied the effects of activating 15-LOX on the AA metabolite network in human polymorphonuclear leucocytes (PMNs) and human whole blood.

RESULTS

Allosteric Site Prediction and Virtual Screening. We hypothesized that enzymatic activity can be modulated by mutations or restraints at distal surface residues that show correlated motions with residues in the active site. A mutual information approach called the "MutInf" method was applied to identify clusters of residues with statistically significant correlations between their dihedral motions.[20] We found several clusters of residues that correlated with the active site (Figure 2a). A suitable binding pocket is also necessary for designing allosteric modulators. Surface cavities were identified and analyzed with the CAVITY program[21,22] (Figure 2b). Cavity **1**, which contained potential allosteric network residues with the highest CAVITY score (Supporting Information (SI), Table S1), was predicted to be the potential allosteric site. Virtual screening was then conducted with the SPECS compound database (November 2009 version for 10 mg; 201 007 compounds) to identify allosteric activators of 15-LOX. A two-step molecular docking scheme was performed, which has been successfully used in discovering active molecules in other systems[23] (see Experimental Section). We selected 175 compounds through this screening method.

Compound Activity Testing. The activity of selected compounds was evaluated with recombinant human 15-LOX in a cell-free assay.[24] One compound activated 15-LOX dose-dependently, and 11 compounds inhibited 15-LOX by more than 50% at 40 μM (SI Table S2). Dose−response profiles were generated for compounds that significantly affected the enzymatic activity of 15-LOX ($EC_{50} < 20$ μM). The activator,
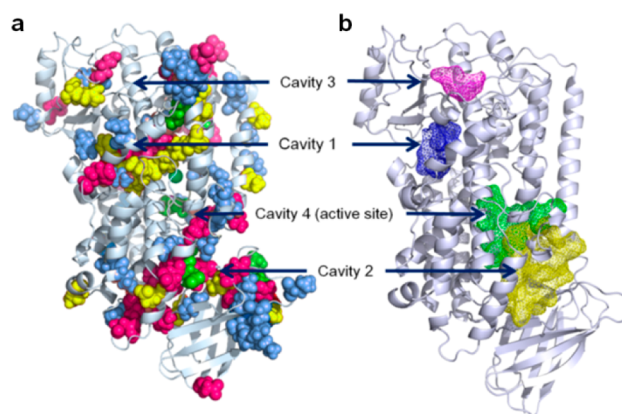

Figure 2. Allosteric site prediction. (a) MutInf identified highly correlated residue couples (correlated residues are shown with the same colored spheres). (b) Pockets identified by the program CAVITY.

(*E*)-1-(7-benzylidene-3-phenyl-3,3a,4,5,6,7-hexahydroindazol-2-yl)-2-(4-methylpiperazin-1-yl)ethanone (PKUMDL_MH_1001, SPECS ID: AO-476/43305824, Figure 3a), enhanced the activity of purified 15-LOX by 85%, with an
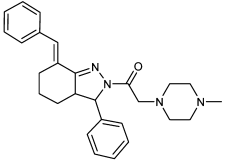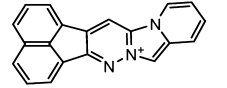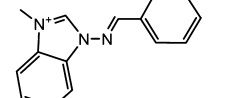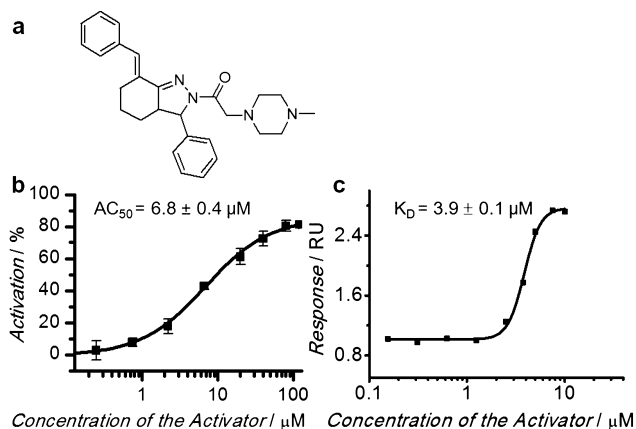

Figure 3. Structures of PKUMDL_MH_1001 and results of cell-free assays. (a) Structures of PKUMDL_MH_1001. Data shown represent the mean ± SEM (*n* = 3). (b) Dose−response curves of cell-free assays. (c) SPR dose−response curves.

AC_{50} value of 6.8 ± 0.4 μM (Figure 3b). Surface plasmon resonance (SPR) demonstrated PKUMDL_MH_1001 bound to 15-LOX in a concentration-dependent manner, with a K_D value of 3.9 ± 0.1 μM (Figure 3c). All these compounds did not match the list of pan assay interference compounds (PAINS),[25] which describes a number of substructural features that appear in frequent hitters (promiscuous compounds) in many biochemical high-throughput screens. This further validated that PKUMDL_MH_1001 is a true hit.

Though our computational screening method only considers how to identify allosteric effectors that bind to target proteins, the allosteric inhibitors and activators that are discovered using the same site can be used to improve our understanding of how 15-LOX is allosterically regulated and facilitate the design of new activators. We found that PKUMDL_MH_1001 possessed a higher positive charge in neutral solution than those of inhibitors. We selected 54 that had binding features similar to those of PKUMDL_MH_1001. (The selection criteria for

Table 1. Activity of Activators in the Cell-Free Assay[a]

Compound	SPECS ID	Structure	Max Activation	K_D determined by SPR (μM)
PKUMDL_MH _1001	AO-476/43 305824		85%	3.9 ± 0.1^{b}
PKUMDL_MH _1024	AQ-405/42 300458		84%	4.4 ± 0.3
PKUMDL_MH _1025	AE-848/305 38061		61%	15.3 ± 0.8

[a]All these compounds did not match the list of PAINS. [b]Errors of K_D were given by fitting response curves.

these 54 compounds are stated in the Experimental Section.) Two activators were identified, acenaphtho[1,2-*e*]pyrido-[1′,2′:3,4]imidazo[1,2-*b*]pyridazin-8-ium (PKUMDL_MH_1024, SPECS ID: AQ-405/42300458) and 1*H*-benzimidazolium, 1-methyl-3-[(phenylmethylene)amino]-, iodide (PKUMDL_MH_1025, SPECS ID: AE-848/30538061) (Table 1). All of the activators were positively charged in neutral solution and did not fully occupy the pocket. The ability to identify new activator compounds based on analysis of the binding feature of 15-LOX activator and inhibitors discovered from virtual screening provides more support to validate the binding modes of the compounds.

Binding Modes of the Allosteric Effectors. To test if these compounds bound to the predicted site, we mutated the predicted key binding residues in 15-LOX according to molecular docking studies. Three single mutations (R242A, E275A, and D277A) and one double mutation (F435A/S440A) were created at the predicted allosteric site (Figure 4a). These mutants possessed different enzymatic activities and showed different responses to PKUMDL_MH_1001 (Figure 4b, SI Table S3). The 15-LOX-activating activities of PKUMDL_MH_1001 were dramatically reduced for mutants R242A (EC$_{50}$ = 51 ± 7 μM, max activation = 400%) and D277A (no activation) compared to that for wild-type 15-LOX

(EC$_{50}$ = 6.8 ± 0.4 μM, max activation = 85%). According to the binding mode given by docking studies, PKUMDL_MH_1001 formed fewer hydrogen bonds with these mutant forms than that observed with wild-type 15-LOX. These results suggest that PKUMDL_MH_1001 binds to the predicted allosteric site.

Influence of the 15-LOX Activator on the AA Network Metabolite Distribution. To further validate the anti-inflammatory activity of PKUMDL_MH_1001, a human whole-blood (HWB) assay was performed to simulate *in vivo* conditions. Fresh human blood was obtained from healthy volunteers who had not received NSAIDs for at least 14 days. We simultaneously stimulated the 5-LOX and COX pathways using lipopolysaccharide and calcium ionophore A23187. Time courses for the formation of major eicosanoids in the AA metabolic network after stimulation were obtained by LC-MS/MS.

Biosynthetic pathways for major eicosanoids in the AA metabolic network and their products were measured as shown in Figure 1. Without any inhibitors or activators, the outputs of the 5-LOX, COX, 12-LOX, and 15-LOX pathways were markedly elevated after stimulation. Changes in eicosanoids after stimulation are shown as heat maps in Figure 5. To evaluate the effects of 15-LOX activation, 100 μM of
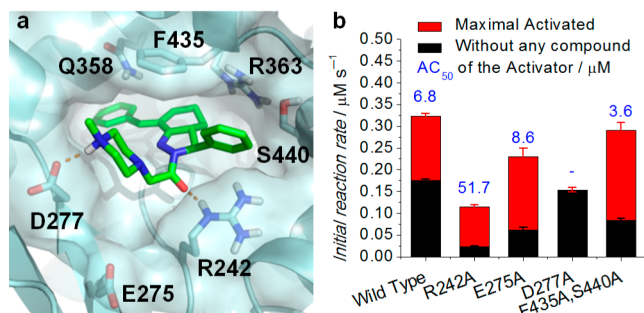

Figure 4. Results of mutation experiments. (a) Binding modes of the PKUMDL_MH_1001. (b) Enzymatic activities and responses to PKUMDL_MH_1001 of 15-LOX mutants. Data shown represent the mean ± SEM (*n* = 3).
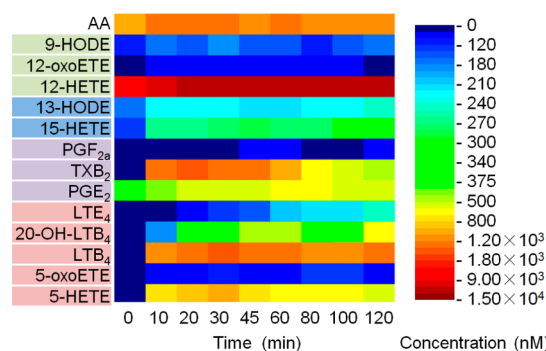

Figure 5. Heat map of dynamic eicosanoid profiles of control group (with no activator or inhibitor).

PKUMDL_MH_1001 was incubated with blood for 20 min before stimulation. The percent changes in eicosanoids after incubating with PKUMDL_MH_1001 are shown in Figure 6a.
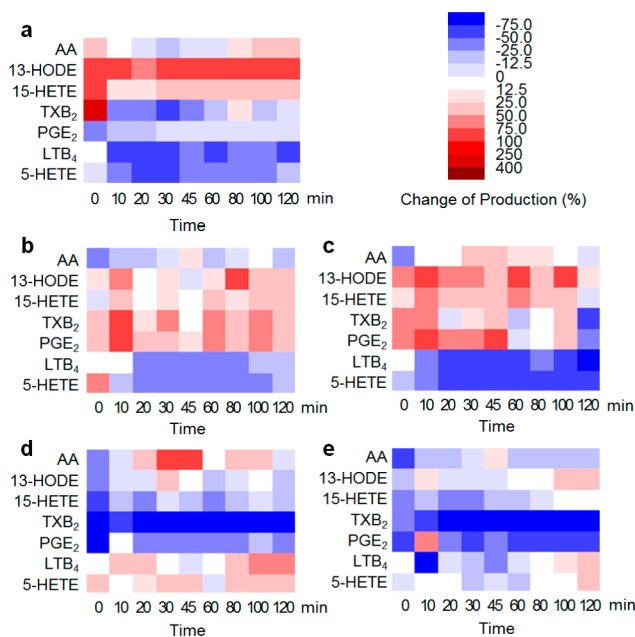

Figure 6. Dynamic eicosanoid production profiles in response to stimulation for 120 min. Changes in eicosanoid production of (a) samples preincubated with the 15-LOX activator, PKUMDL_MH_1001, (b) samples preincubated with the 5-LOX inhibitor, Zileuton, (c) samples preincubated with a combination of PKUMDL_MH_1001 and Zileuton, (d) samples preincubated with the COX inhibitor, Flurbiprofen, and (e) samples preincubated with a combination of Flurbiprofen and PKUMDL_MH_1001. Change in production was defined as the normalized concentration of eicosanoid relative to that in the control set minus 1 and multiplied by 100%.

(Absolute amounts of eicosanoids formed and standard error of means are given in SI Table S4.) The production of 15-HETE and 13-HODE increased by $33 \pm 8\%$ and $95 \pm 10\%$, respectively, relative to the control during the 120 min time period (this value is equivalent to the percent change in the area under the concentration−time curve divided by 120 min). On the other hand, addition of the 15-LOX activator reduced the levels of products from the 5-LOX and COX pathways. PKUMDL_MH_1001 reduced the formation of leukotriene B_4 (LTB_4, 5-LOX pathway) and Thromboxane B_2 (TXB_2, COX pathway) by $52 \pm 13\%$ and $27 \pm 13\%$, respectively.

To verify that this phenomenon was caused by 15-LOX activation, we tested the effects of PKUMDL_MH_1001 on other enzymes in the AA network. PKUMDL_MH_1001 did not demonstrate activity against COX-1/COX-2, 5-LOX, or leukotriene A_4 hydrolase (LTA_4H) in cell-free assays (less than 5% inhibition or activation at 100 μM) and only slightly inhibited cytosolic phospholipase A2 (cPLA2) (inhibition = 20% at 100 μM) and mPGES (IC_{50} = 20 ± 1 μM, inhibition = 63% at 100 μM). We also confirmed that PKUMDL_MH_1001 could activate 15-LOX in human PMNs (SI Figure S1). Moreover, when a 5-LOX inhibitor (Zileuton) was added in HWB which completely shut off the 5-LOX pathway, PKUMDL_MH_1001 could still elevate the production of 15-HETE (SI Figure S2). These results suggest

that the effects of PKUMDL_MH_1001 in the AA network were predominantly caused by 15-LOX activation.

Combinations of 15-LOX Activator with 5-LOX or COX Inhibitors. We also studied the effects of combining the 15-LOX activator with the 5-LOX or COX inhibitor. When 5-LOX inhibitor (Zileuton, 2 μM) was used, the production of 5-HETE and LTB_4 (Figure 6b) in blood was decreased with average values of $35 \pm 5\%$ and $28 \pm 4\%$, respectively. In contrast, the levels of TXB_2 and prostaglandin E_2 (PGE_2) were increased by 1.5 times and 1.4 times, respectively. The addition of PKUMDL_MH_1001 to the 5-LOX inhibitor further reduced the production of 5-HETE and LTB_4 to $59 \pm 5\%$ and $54 \pm 5\%$, respectively (Figure 6b,c). Although TXB_2 and PGE_2 concentrations were higher than that of the control, the levels of these metabolites were lower in the combination group than that in the 5-LOX inhibitor alone group (Figure 6b,c). The levels of 15-HETE and 13-HODE were increased with the combination by $36 \pm 5\%$ and $67 \pm 9\%$ on average, respectively, which were greater than that with the 5-LOX inhibitor alone. Similarly, the addition of PKUMDL_MH_1001 with a COX inhibitor (Flurbiprofen, 2 μM) further increased COX inhibition and decreased the production of 5-HETE and LTB_4. The combination also slightly elevated the levels of 15-HETE and 13-HODE compared to using COX inhibitor alone (Figure 6d,e). In summary, addition of the 15-LOX activator to the 5-LOX or COX inhibitor resulted in more efficient modulation of the target pathways. Side effects caused by inhibitors will be avoided with the activator, because AA is expected to be shunted toward anti-inflammatory pathways.

■ DISCUSSION

Pharmacological activation of enzymes requires interactions with allosteric sites, because active-site competitors are generally inhibitory. In a previous study, we developed an approach to identify allosteric sites in proteins based on the coarse-grained two-state Gō model.[26] This method successfully predicted several new allosteric sites that led to the discovery of novel allosteric inhibitors of *Escherichia coli* phosphoglycerate dehydrogenase. However, this method requires that both the bound and unbound structures are known and the structures should be different at the level of the residue-to-residue contacts. In the present study, we used a protein dynamics-based allosteric-site prediction approach together with a pocket-finding method to predict potential allosteric sites that are suitable targets for pharmacological regulators. One advantage of the present approach is that we can predict an allosteric site without prior knowledge of the active conformation or co-crystal structure of the ligand bound to the target site. This is an important advantage, as this information is rarely available for the allosteric sites of enzymes. Another advantage of our approach is that structure-based drug design methods, such as virtual screening, fragment-based, or *de novo* design, can be directly applied to identify allosteric regulators by considering the ligand-binding abilities of potential allosteric sites.

Adding or removing a posttranslational modification of a protein can be seen as a covalent allosteric regulation[27] and often involves changes in charge. In a previous study,[28] negatively charged compounds which mimic phosphorylation have been successfully designed to activat protein kinase PDK1 by binding to an allosteric site. In our study, all activators carry positive charge and the single mutation R242A has a significantly lowered enzymatic activity, which can be rescued by binding to the positively charged activator. These results

suggest that change in local charge at the predicted allosteric site can affect the activity of 15-LOX and binding of PKUMDL_MH_1001 gives an allosteric perturbation similar to posttranslational modification. Of course, further experimental studies are needed to understand the mechanism

In many cases,[29−31] a slight enhancement in enzymatic activity may be sufficient to induce biological effects. In the present study, PKUMDL_MH_1001 activated 15-LOX by about 30% in the HWB assay. However, it significantly altered the flux distribution in the AA metabolic network as shown in the metabolite analysis experiments. The activator simultaneously decreased the production of LTs and PGs, whereas selective inhibitors caused an inevitable increase in other pro-inflammatory metabolites. Our experimental results in cell assays demonstrate that the 15-LOX activator can improve the control of inflammation due to reduced production of pro-inflammatory products and increased production of 15-HETE. Our discovery of the 15-LOX activator should aid in the discovery of new anti-inflammatory drug combinations that are safe and effective. In addition to their potential therapeutic applications, our activators are valuable tools in understanding the biological consequences of enzyme activation within the signaling pathway.

■ EXPERIMENTAL SECTION

Comparative Modeling. We used the PRIME (Schrodinger, Inc.) comparative modeling environment to construct a model of human 15-LOX from rabbit 15S-lipoxygenase (PDB code: 2P0M, 81% sequence identity, similarity = 90%). We retained the metal iron and the geometries of the conserved side chains. In addition, we optimized and minimized the side chains of non-conserved residues.

Molecular Dynamics Simulations. We performed molecular dynamics simulations in explicit solvent with the Desmond[32] software package and OPLS-AA/SPC force field.[33] The protein was placed in an orthorhombic simulation with a buffer of 10 Å on each side. Na^+ and Cl^- ions were added to neutralize the system, and then 0.05 M NaCl was added. Minimization was initially performed with the solute positions restrained at 50 kcal/(mol·Å) for 2000 steps. The solute positions were unrestrained, and minimization proceeded for another 2000 steps. Next, heavy atoms in the solute were restrained at 50 kcal/(mol·Å). NVT molecular dynamic simulations were performed at 10 K for 12 ps. This was followed by NPT equilibration at 10 K for 12 ps. Then, the system was simulated for another 34 ps at 300 K with the same settings. Finally, restraints on heavy atoms were removed, and the system was simulated for an additional 24 ps at 300 K with a thermostat-relaxation rate of 0.1 ps^{-1} and barostat-relaxation rate of 2 ps^{-1}.

After minimization and equilibration, multiple (different random seed) production runs of 10 ns were performed on each system with the Martyna−Tobias−Klein integrator[34] at 300 K and 1 atm. Snapshots were taken every 1.0 ps. Production runs were collected as follows. Six production runs were performed for 10 ns each and were used for the MutInf calculations. Additional sampling was performed to identify open pockets and for clustering. More production runs of up to 9 ns each were initiated from 10 ns equilibration checkpoints. Overall, 232 ns of production molecular dynamics was collected. Detailed procedures are described in the SI.

MutInf Calculations. To identify novel allosteric sites for activation of 15-LOX, we used the previously reported MutInf program[20] for the initial set of six 10 ns production runs. This method analyzes conformational ensembles, such as those from molecular dynamic simulations, to identify statistically significant correlated motions based on mutual information metrics, which thermodynamically quantify correlated motions. To identify novel allosteric sites, we hierarchically clustered residues that exhibited similar magnitudes of mutual information using the heat map function in the R statistical package as previously described.[20]

Clustering and Identification of Significantly Populated Open-Pocket Conformations. All production simulations were combined for clustering purposes, and clustering was performed in Gromacs with QT clustering ("cluster−method gromos")[35] and a cutoff of 0.5 Å. Representative conformations from the top 30 clusters were inspected. Six open-pocket conformations were selected and aligned using all-atoms in Pymol (Schrodinger, Inc.) with the "intra_fit" command.

CAVITY Analysis. The structure of human 15-LOX was analyzed by the program CAVITY[21,22] using the default parameters. The predicted maximal pK_d values of the identified pockets in this protein are listed in SI Table S1.

Virtual Screening. We clustered the conformations of Cavity **1** that were obtained from the molecular dynamics simulation trajectories and identified a number of populated, open-pocket conformations. Representative conformations from six highly populated open conformations were used for subsequent docking studies. All compounds in the SPECS compound database (November 2009 version for 10 mg; 201 007 compounds) were docked into the allosteric pocket with the rigid-body docking approach of the DOCK 6.1[36] program using the default parameters. Twenty thousand compounds with the lowest estimated K_i values were selected from each of the six pocket conformations for the next step. The AutoDock step of virtual screening was performed with the Lamarckian genetic algorithm using the following parameters: number of genetic algorithm runs, 20; number of individuals in population, 150; maximum number of energy evaluations, 1 750 000; maximum of generations, 27 000. Size of grid box was 60 × 60 × 60 (number of grid points in *xyz*-coordinates). Center of grid box was at the center of Cavity **1** (key residues of Cavity **1**: 239, 240, 242, 280, 354, 358, 363, 435, and 436).The first 500 compounds with the lowest estimated K_i values were selected from each of the six pocket conformations. The binding conformations of these compounds were exported and manually evaluated according to the following criteria: (1) The compound formed at least two hydrogen bonds. (2) The compound was not a polypeptide. (3) The compound did not contain metal atoms. Correlation analysis between experimental pIC_{50} and calculated pK_d is given in SI Figure S3. Ranks of identified hits in virtual screen are given in SI Table S5.

Choosing Compounds That Have a Binding Mode Similar to That of PKUMDL_MH_1001. The top 3000 compounds from virtual screening were rescored by Glide (Schrodinger, Inc.), and their interactions with residues within 12 Å were calculated. The difference between these interactions and that of PKUMDL_MH_1001 was defined as follows:

$$\text{Difference of Interactions} = \sum \left(\text{Score}_{\text{compound x},i} - \text{Score}_{\text{compound 1},i} \right)^2 \qquad (1)$$

where "Score" is the Glide-Score term of a compound interacting with certain residues and i is the residue number. A scatter map was drawn using the difference between Coulombic and van der Waals interaction scores as the *y*-axis and the difference of the hydrogen-bond scores as the *x*-axis (SI Figure S4). The compounds that had binding modes similar to that of PKUMDL_MH_1001 clustered around the origin of the scatter map. Compounds in the cluster were selected for *in vitro* testing.

Chemicals and Reagents. The purities of the compounds in the SPECS database exceed 90%; most compounds are more than 95% pure (confirmed by the supplier, using NMR, LS-MS, or both; data available through the website.; for our hits, PKUMDL_MH_1001, PKUMDL_MH_1024, and PKUMDL_MH_1025, NMR and LC-MS data are provided in the SI). PD146176 and standard compounds for LC-MS/MS were purchased from Cayman Chemical (Ann Arbor, MI, USA). Zileuton was purchased from Tocris Bioscience (Bristol, UK). Flurbiprofen and Nordihydroguaiaretic acid were purchased from Alfa Aesar. Calcium ionophore A23187 was obtained from Sigma-Aldrich (St. Louis, MO, USA). Heparin was obtained from J&K Chemical (Beijing, China). Acetonitrile (ABSOLV grade) was supplied by Tedia Company (Fairfield, OH, USA). Ampicillin, clarithromycin, isopropyl

β-thiogalactoside, dithiothreitol, ethylenediaminetetraacetic acid, phenylmethanesulfonyl fluoride, and dimethyl sulfoxide (DMSO) were from Amresco (Solon, OH, USA). The Symmetry C18 reverse-phase column (3.5 μm, 2.1 mm × 150 mm) and Oasis solid-phase-extraction cartridge (30 mm, 1 cm³/30 mg) were purchased from Waters Corp. (Milford, MA, USA). Water was purified with a Milli-Q Reagent Water System (Millipore, Billerica, USA).

Molecular Cloning, Protein Expression, and Purification of 15-LOX. Wild-type human *15-LOX* was amplified from a cDNA clone (MGC:34638 IMAGE:5179700; Source BioScience). The amplified fragments of *15-LOX* were ligated into the pET-28a vector with T4 DNA ligase. The resulting plasmid, pET-*15LOX*-h28, encoded the 15-LOX protein with an N-terminal His6 tag. Mutations were introduced into *15-LOX* with the QuikChange site-directed mutagenesis kit (Stratagene) with pET-*15LOX*-h28 as a template.

pET-*15LOX*-h28 and mutants were transformed into *E. coli* strain Rosetta <DE3> for expression of His6-tagged 15-LOX (His6-15LOX) and His6-tagged mutant proteins. Cells were cultured at 37 °C in LB media containing Fe^{2+} (50 μM), kanamycin (34 μg mL^{-1}), and chloramphenicol (30 μg mL^{-1}). At an A600 of about 1.0, isopropyl β-D-thiogalactopyranoside was added to a final concentration of 0.5 mM. Cells were grown for an additional 12 h at 22 °C, harvested, resuspended in lysis buffer [Tris-HCl (50 mM, pH 8.0), NaCl (100 mM), 1,4-dithiothreitol (1 mM), and phenylmethylsulfonyl fluoride (1 mM)], and lysed by ultrasonic treatment.

The supernatant of the lysate was applied to a nickel−nitrilotriacetic acid column (HisTrap HP; GE Healthcare) and eluted with Tris-HCl buffer (pH 8.0) containing imidazole (200 mM). The eluted enzyme was further purified using an anion-exchange column (Q Trap HP; GE Healthcare). All buffers were degassed before use, and the entire purification procedure was performed at 4 °C.

The purities of the protein samples (>95%, SI Figure S5) were confirmed by SDS/PAGE on a polyacrylamide gel (10%, w/v) with a mini-vertical gel system (Bio-Rad). Bands were visualized by Coomassie Brilliant Blue staining. Protein concentrations were determined by measuring absorbance at 280 nm with an extinction coefficient of 1.20×10^5 M^{-1} cm^{-1}. Detailed procedures are described in the SI.

Activation and Inhibition of 15-LOX in a Cell-Free Assay. Lipoxygenase rates were assessed by measuring the formation of product at 235 nm (ε = 25 000 M^{-1} cm^{-1}).[24] The enzyme was added to quartz 96-well microtiter plates in sodium phosphate buffer (100 mM, pH 7.4) and incubated with a compound (dissolved in DMSO) at room temperature for 1 min. Reactions were initiated by adding the substrate, AA. Absorbance of 15-HpETE was monitored on a plate reader (Synergy, Biotek). The IC$_{50}$ and AC$_{50}$ calculations were performed with 50 μM AA and 1% DMSO. The initial reaction rates at different concentrations of compound were used to determine EC$_{50}$ concentrations, which were calculated with a four-parameter logistical model of log dose against percentage inhibition or activation and were obtained from three sets of experiments. For Compound Activity Testing, the initial reaction rate without any compound was kept about 0.17 μM s^{-1} (9.3 O.D. h^{-1}). We also digested His6-15LOX with thrombin (Sigma) to remove the His6 tag and test the enzymatic activity using this method. No significant difference was observed (SI Figure S6). Therefore, all data from in the cell-free assay was conducted using His6-15LOX.

Inhibition of 5-LOX in a Cell-Free Assay. The enzymatic activity of 5-LOX was determined by monitoring the oxidation of the substrate, H$_2$DCFDA, to the highly fluorescent 2′,7′-dichlorofluorescein product during the catalytic reaction mediated by 5-LOX as reported.[37] The human 5-LOX protein was prepared as previous reported.[38] Briefly, the reactions were initiated by adding AA as the substrate and monitoring excitation at 500 nm and emission at 520 nm on a multi-wall fluorometer (Synergy4, BIOTEK). Fluorescence signals were recorded for 5 min. Inhibition of 5-LOX was measured in a similar manner as that of 15-LOX. Detailed procedures are described in the SI.

Inhibition of cPLA2 in a Cell-Free Assay. The enzymatic activity of cPLA2 was determined by monitoring the hydrolysis of the substrate, 7-hydroxycoumarinyl-γ-linolenate or 2-oxo-2*H*-chromen-6-yl (6Z,9Z,12Z)-octadeca-6,9,12-trienoate, to the highly fluorescent product, 7-hydroxycoumarin, during the catalytic reaction mediated by cPLA2 as described previously.[39] The reactions were initiated by adding purified human cPLA2 (final concentration 1 μg/mL) and monitoring excitation at 355 nm and emission at 460 nm on a multi-wall fluorometer (Synergy4, BIOTEK). Fluorescence signals were recorded for 84 min. Inhibition of cPLA2 was measured in a similar manner as that of 15-LOX.

Inhibition of mPGES-1 in a Cell-Free Assay. The enzymatic activity of mPGES-1 was determined by assessing conversion of PGH$_2$ to PGE$_2$.[40,41] Production of PGE$_2$ in the reaction mixture was measured with the PGE2 EIA kit (Cayman Chemical). Inhibition was measured in a similar manner as that of 15-LOX.

Inhibition of COX-2 in a Cell-Free Assay. The enzymatic activities of COX family members were determined by spectrophotometrically monitoring the oxidation of N,N,N′,N′-tetramethyl-*p*-phenylenediamine during the conversion of PGG$_2$ to PGH$_2$.[42] Inhibition was measured in a similar manner as that of 15-LOX.

Inhibition of LTA$_4$H in a Cell-Free Assay. LTA$_4$H hydrolase activity was measured by monitoring the formation of LTB$_4$ with an enzyme-linked immunosorbent assay.[43] Inhibition was measured in a similar manner as that of 15-LOX.

SPR Experiments. The binding affinity of compounds toward 15-LOX was assayed using the SPR-based Biacore T200 instrument. 15-LOX was immobilized on a CM5 sensor chip by using standard amine-coupling at 25 °C with running buffer PBS-P (20 mM phosphate buffer, 2.7 mM NaCl, 137 mM KCl, 0.05% surfactant P-20, pH 7.4) as described previously.[44] In the direct binding experiments between 15-LOX and compounds, 15-LOX immobilization level was fixed at 800 response units (RU), and then different concentrations of compounds containing 5% DMSO were serially injected into the channel to evaluate binding affinity. Regeneration was achieved by extended washing with the running buffer after each sample injection. The equilibrium dissociation constants (K$_D$) of compounds were obtained by fitting binding response units to Hill equation. The SPR dose−response curves of activators with immobilized 15-LOX are shown in SI Figure S7.

Induction of an Inflammatory Reaction in the AA Metabolic Network in Human Whole Blood. Fresh human blood was obtained from healthy volunteers who had not received NSAIDs for at least 14 days. Coagulation was prevented with heparin (J&K Chemical LTD) at 10 UI/mL, and 0.5 mL of blood was immediately divided into a series of PP tubes. Blood samples were pre-incubated for 20 min at 37 °C with either vehicle (DMSO) or various concentrations of test compounds in DMSO solution. LPS (Sigma) was added to blood at 100 μg/mL followed by incubation for 24 h at 37 °C. The calcium ionophore A23187 was then added at a final concentration of 20 μg/mL. The incubation was terminated at various time points by freezing the samples in liquid nitrogen.

Sample Preparation. Human blood samples were lysed by three cycles of freezing and thawing. The lysate was diluted with 0.1% formic acid (v/v) in water to a final 2 mL volume. PGB$_2$ was added to the diluted sample as an internal standard. Eicosanoids were extracted with Oasis HLB solid-phase-extraction cartridges. The cartridges were preconditioned with 2 mL of methanol and equilibrated with 2 mL of H$_2$O. The plasma samples were centrifuged and the supernatants were placed on HLB cartridges. The cartridges were washed with 2 mL of water containing 5% methanol and 0.1% formic acid (v/v). The eicosanoids were eluted with 1 mL of methanol and 0.1% formic acid (v/v). The samples were evaporated under a stream of nitrogen and reconstituted with 100 μL of methanol before LC-MS analysis.

LC-MS/MS Method. LC separation was performed with a Shimadzu Prominence UFLC XR (Shimadzu Corporation). The multiple-reaction-monitoring (MRM) spectra were obtained with a QTRAP 5500 mass spectrometer (AB SCIEX) equipped with an ESI source. A Waters Symmetry reverse-phase C18 column (2.1 mm × 150 mm, 3.5 μm) was used for the LC separation. The mobile phase consisted of water (A) containing 0.1% formic acid and acetonitrile (B) containing 0.1% formic acid. The flow rate was 0.3 mL min^{-1}. The

solvent-gradient elution was changed as follows: 0 min, 30% B; 6.5 min, 36.5% B; 6.5 min, 38.9% B; 10.0 min, 40% B; 16.5 min, 56% B; 27.5 min, 56% B; 31.9 min, 78% B; 32.0 min, 90% B; 38.0, 90% B; followed by re-equilibration from 38 to 45 min. Twenty milliliter portions of each sample were injected into the HPLC system. All data were acquired in negative-ion mode. Up to 35 eicosanoids were monitored, including TXB_2, $PGF_{2\alpha}$, $PGF_{1\alpha}$, PGE_2, PGD_2, LXB_4, LXA_4, LTE_4, LTB_4, 14,15-leukotriene C_4 (EXC_4), AA, 9-HODE, 8-HETE, 8,9-epoxyeicosatrienoic acid (EET), 8,9-dihydroxyeicosatrienoic acid (DHET), 5-oxoeicosatetraenoic acid (oxoETE), 5-HETE, 5,6-EET, 5,6-DHET, 20-hydroxy-PG $F_{2\alpha}$, 20-hydroxy-PGE_2, 20-hydroxy-LTB_4, 20-HETE, 19-HETE, 18-HETE, 17-HETE, 16-HETE, 15-oxoETE, 15-HETE, 14,15-EET, 14,15-DHET, 13-HODE, 12-oxoETE, 12-HETE, 11,12-DHET, and internal standards (PGB_2 and 5-HETE-d_8). Optimized LC-MS/MS parameters for the analysis of eicosanoids are listed in SI Table S6.

Influence of the 15-LOX Activator in Human Polymorphonuclear Leucocytes. Following the reported procedure,[3] human PMNs were isolated from the venous blood of healthy volunteers who had not ingested any aspirin-like compounds in the preceding week. PMNs were pre-incubated with vehicle (menthol), Zileuton (an inhibitor of 5-LOX), and PKUMDL_MH_1001 at 37 °C for 15 min, respectively. To stimulate the PMNs, 10 μM A23187, 2 mM Ca^{2+}, and 2 mM Mg^{2+} were added for 1 h at 37 °C. Incubations were terminated by the addition of cold menthol (700 μL of menthol was added into 300 μL of reaction solution). PGB_2 was added as an internal standard. The upper solvent was evaporated under a stream of nitrogen, and the residue was dissolved in 150 μL of methanol before LC-MS analysis.

■ ASSOCIATED CONTENT

Ⓢ Supporting Information

The Supporting Information is available free of charge on the ACS Publications website at DOI: 10.1021/acs.jmedchem.5b01011.

Tables S1–S6 and Figures S1–S7, including correlation analysis between experimental pIC_{50} and calculated pK_d and ranks of identified hits in virtual screen; supplementary methods; and NMR and MS spectra of PKUMDL_MH_1001, PKUMDL_MH_1024, and PKUMDL_MH_1025 (PDF)

Molecular formula strings (CSV)

■ AUTHOR INFORMATION

Corresponding Author

*Telephone: (+86)10-62757486. Fax: (+86)10-62751725. E-mail: lhlai@pku.edu.cn.

Author Contributions

L.L., H.M., and C.L.M. conceived and designed the experiments. H.M. performed virtual screening, all the 15-LOX experimental studies, and molecular dynamics simulations of the allosteric effectors. C.L.M. performed molecular dynamics simulations, MutInf calculations, and virtual screening. Z.D. performed data analysis. K.L. and X.Z. performed purification of 15-LOX. S.H. and E.S. performed cell-free assays of mPGES, COX, and LTA_4H. H.M., C.L.M., Y.L., and L.L. analyzed the data. H.M., C.L.M., and L.L. wrote the paper.

Notes

The authors declare no competing financial interest.

■ ABBREVIATIONS USED

15-lipoxygenase (15-LOX); arachidonic acid (AA); leukotrienes (LTs); prostaglandins (PGs); 5-lipoxygenase (5-LOX); cyclooxygenase (COX); lipoxins (LXs); human reticulocyte 15-lipoxygenase (15-LOX type 1, 15-LOX-1); 15-hydroxyeicosatetraenoic acid (15-HETE); 13-hydroxyoctadecadienoic acid (13-HODE); polymorphonuclear leucocytes (PMNs); surface plasmon resonance (SPR); pan assay interference compounds (PAINS); human whole-blood assay (HWB); leukotriene A_4 hydrolase (LTA_4H); cytosolic phospholipase A2 (cPLA2); leukotriene B_4 (LTB_4); Thromboxane B_2 (TXB_2); prostaglandin E_2 (PGE_2); 14,15-leukotriene C_4 (EXC_4); epoxyeicosatrienoic acid (EET); dihydroxyeicosatrienoic acid (DHET); oxoeicosatetraenoic acid (oxoETE)

■ REFERENCES

(1) Zorn, J. A.; Wells, J. A. Turning enzymes ON with small molecules. *Nat. Chem. Biol.* **2010**, *6*, 179–188.

(2) Khanapure, S. P.; Garvey, D. S.; Janero, D. R.; Letts, L. G. Eicosanoids in inflammation: Biosynthesis, pharmacology, and therapeutic frontiers. *Curr. Top. Med. Chem.* **2007**, *7*, 311–340.

(3) Yang, K.; Ma, W. Z.; Liang, H. H.; Qi, O. Y.; Tang, C.; Lai, L. H. Dynamic simulations on the arachidonic acid metabolic network. *PLoS Comput. Biol.* **2007**, *3*, 523–530.

(4) Rainsford, K. D. Leukotrienes in the Pathogenesis of Nsaid-Induced Gastric and Intestinal Mucosal Damage. *Agents Actions* **1993**, *39*, C24–C26.

(5) He, C.; Wu, Y. R.; Lai, Y. Q.; Cai, Z. W.; Liu, Y.; Lai, L. H. Dynamic eicosanoid responses upon different inhibitor and combination treatments on the arachidonic acid metabolic network. *Mol. BioSyst.* **2012**, *8*, 1585–1594.

(6) Serhan, C. N.; Hamberg, M.; Samuelsson, B. Lipoxins - Novel Series of Biologically-Active Compounds Formed from Arachidonic-Acid in Human-Leukocytes. *Proc. Natl. Acad. Sci. U. S. A.* **1984**, *81*, 5335–5339.

(7) Leslie, M. Inflammation's STOP SIGNALS. *Science* **2015**, *347*, 18–21.

(8) Kuhn, H.; O'Donnell, V. B. Inflammation and immune regulation by 12/15-lipoxygenases. *Prog. Lipid Res.* **2006**, *45*, 334–356.

(9) Huang, J. T.; Welch, J. S.; Ricote, M.; Binder, C. J.; Willson, T. M.; Kelly, C.; Witztum, J. L.; Funk, C. D.; Conrad, D.; Glass, C. K. Interleukin-4-dependent production of PPAR-gamma ligands in macrophages by 12/15-lipoxygenase. *Nature* **1999**, *400*, 378–382.

(10) Straus, D. S.; Glass, C. K. Anti-inflammatory actions of PPAR ligands: new insights on cellular and molecular mechanisms. *Trends Immunol.* **2007**, *28*, 551–558.

(11) Chan, M. M.; Evans, K. W.; Moore, A. R.; Fong, D. Peroxisome Proliferator-Activated Receptor (PPAR): Balance for Survival in Parasitic Infections. *J. Biomed. Biotechnol.* **2010**, *2010*, 1–9.

(12) Yang, K.; Bai, H.; Ouyang, Q.; Lai, L.; Tang, C. Finding multiple target optimal intervention in disease-related molecular network. *Mol. Syst. Biol.* **2008**, *4*, 228.

(13) Engel, M.; Hindie, V.; Lopez-Garcia, L. A.; Stroba, A.; Schaeffer, F.; Adrian, I.; Imig, J.; Idrissova, L.; Nastainczyk, W.; Zeuzem, S.; Alzari, P. M.; Hartmann, R. W.; Piiper, A.; Biondi, R. M. Allosteric activation of the protein kinase PDK1 with low molecular weight compounds. *EMBO J.* **2006**, *25*, 5469–5480.

(14) Tappan, E.; Chamberlin, A. R. Activation of protein phosphatase 1 by a small molecule designed to bind to the enzyme's regulatory site. *Chem. Biol.* **2008**, *15*, 167–174.

(15) McCarthy, A. R.; Hollick, J. J.; Westwood, N. J. The discovery of nongenotoxic activators of p53: Building on a cell-based high-throughput screen. *Semin. Cancer Biol.* **2010**, *20*, 40−45.

(16) Hardy, J. A.; Lam, J.; Nguyen, J. T.; O'Brien, T.; Wells, J. A. Discovery of an allosteric site in the caspases. *Proc. Natl. Acad. Sci. U. S. A.* **2004**, *101*, 12461−12466.

(17) Cool, B.; Zinker, B.; Chiou, W.; Kifle, L.; Cao, N.; Perham, M.; Dickinson, R.; Adler, A.; Gagne, G.; Iyengar, R.; Zhao, G.; Marsh, K.; Kym, P.; Jung, P.; Camp, H. S.; Frevert, E. Identification and characterization of a small molecule AMPK activator that treats key components of type 2 diabetes and the metabolic syndrome. *Cell Metab.* **2006**, *3*, 403−416.

(18) Whitman, S.; Gezginci, M.; Timmermann, B. N.; Holman, T. R. Structure-activity relationship studies of nordihydroguaiaretic acid inhibitors toward soybean, 12-human, and 15-human lipoxygenase. *J. Med. Chem.* **2002**, *45*, 2659−61.

(19) Andersson, E.; Schain, F.; Svedling, M.; Claesson, H. E.; Forsell, P. K. A. Interaction of human 15-lipoxygenase-1 with phosphatidyli-nositol bisphosphates results in increased enzyme activity. *Biochim. Biophys. Acta, Mol. Cell Biol. Lipids* **2006**, *1761*, 1498−1505.

(20) McClendon, C. L.; Friedland, G.; Mobley, D. L.; Amirkhani, H.; Jacobson, M. P. Quantifying Correlations Between Allosteric Sites in Thermodynamic Ensembles. *J. Chem. Theory Comput.* **2009**, *5*, 2486−2502.

(21) Yuan, Y. X.; Pei, J. F.; Lai, L. H. LigBuilder 2: A Practical de Novo Drug Design Approach. *J. Chem. Inf. Model.* **2011**, *51*, 1083−1091.

(22) Yuan, Y.; Pei, J.; Lai, L. Binding site detection and druggability prediction of protein targets for structure-based drug design. *Curr. Pharm. Des.* **2013**, *19*, 2326−33.

(23) He, S.; Li, C.; Liu, Y.; Lai, L. Discovery of highly potent microsomal prostaglandin e2 synthase 1 inhibitors using the active conformation structural model and virtual screen. *J. Med. Chem.* **2013**, *56*, 3296−309.

(24) Mogul, R.; Holman, T. R. Inhibition studies of soybean and human 15-lipoxygenases with long-chain alkenyl sulfate substrates. *Biochemistry* **2001**, *40*, 4391−7.

(25) Baell, J. B.; Holloway, G. A. New Substructure Filters for Removal of Pan Assay Interference Compounds (PAINS) from Screening Libraries and for Their Exclusion in Bioassays. *J. Med. Chem.* **2010**, *53*, 2719−2740.

(26) Qi, Y. F.; Wang, Q.; Tang, B.; Lai, L. H. Identifying Allosteric Binding Sites in Proteins with a Two-State G(o)over-bar Model for Novel Allosteric Effector Discovery. *J. Chem. Theory Comput.* **2012**, *8*, 2962−2971.

(27) Honn, K. V.; Cicone, B.; Skoff, A. Prostacyclin: a potent antimetastatic agent. *Science* **1981**, *212*, 1270−2.

(28) Smith, J. B.; Araki, H.; Lefer, A. M. Thromboxane A2, prostacyclin and aspirin: effects on vascular tone and platelet aggregation. *Circulation* **1980**, *62*, V19−25.

(29) Cardenas, M. L.; Cornishbowden, A. Characteristics Necessary for an Interconvertible Enzyme Cascade to Generate a Highly Sensitive Response to an Effector. *Biochem. J.* **1989**, *257*, 339−345.

(30) Goldbeter, A.; Koshland, D. E. Sensitivity Amplification in Biochemical Systems. *Q. Rev. Biophys.* **1982**, *15*, 555−591.

(31) Szedlacsek, S. E.; Cardenas, M. L.; Cornishbowden, A. Response Coefficients of Interconvertible Enzyme Cascades Towards Effectors That Act on One or Both Modifier Enzymes. *Eur. J. Biochem.* **1992**, *204*, 807−813.

(32) Bowers, K. J.; Chow, E.; Xu, H.; Dror, R. O.; Eastwood, M. P.; Gregersen, B. A.; Klepeis, J. L.; Kolossvary, I.; Moraes, M. A.; Sacerdoti, F. D.; Salmon, J. K.; Shan, Y.; Shaw, D. E. Scalable Algorithms for Molecular Dynamics Simulations on Commodity Clusters. In *Proceedings of the ACM/IEEE Conference on Super-computing (SC06)*, Tampa, Florida, 2006.

(33) Kaminski, G. A.; Friesner, R. A.; Tirado-Rives, J.; Jorgensen, W. L. Evaluation and reparametrization of the OPLS-AA force field for proteins via comparison with accurate quantum chemical calculations on peptides. *J. Phys. Chem. B* **2001**, *105*, 6474−6487.

(34) Martyna, G. J.; Tobias, D. J.; Klein, M. L. Constant-Pressure Molecular-Dynamics Algorithms. *J. Chem. Phys.* **1994**, *101*, 4177−4189.

(35) Daura, X.; Gademann, K.; Jaun, B.; Seebach, D.; van Gunsteren, W. F.; Mark, A. E. Peptide folding: When simulation meets experiment. *Angew. Chem., Int. Ed.* **1999**, *38*, 236−240.

(36) Lang, P. T.; Brozell, S. R.; Mukherjee, S.; Pettersen, E. F.; Meng, E. C.; Thomas, V.; Rizzo, R. C.; Case, D. A.; James, T. L.; Kuntz, I. D. DOCK 6: Combining techniques to model RNA-small molecule complexes. *RNA* **2009**, *15*, 1219−1230.

(37) Pufahl, R. A.; Kasten, T. P.; Hills, R.; Gierse, J. K.; Reitz, B. A.; Weinberg, R. A.; Masferrer, J. L. Development of a fluorescence-based enzyme assay of human 5-lipoxygenase. *Anal. Biochem.* **2007**, *364*, 204−12.

(38) Wu, Y. R.; He, C.; Gao, Y.; He, S.; Liu, Y.; Lai, L. H. Dynamic Modeling of Human 5-Lipoxygenase-Inhibitor Interactions Helps To Discover Novel Inhibitors. *J. Med. Chem.* **2012**, *55*, 2597−2605.

(39) McKew, J. C.; Foley, M. A.; Thakker, P.; Behnke, M. L.; Lovering, F. E.; Sum, F. W.; Tam, S.; Wu, K.; Shen, M. W. H.; Zhang, W.; Gonzalez, M.; Liu, S. H.; Mahadevan, A.; Sard, H.; Khor, S. P.; Clark, J. D. Inhibition of cytosolic phospholipase A2 alpha: Hit to lead optimization. *J. Med. Chem.* **2006**, *49*, 135−158.

(40) Haeggstrom, J. Z. Leukotriene A4 hydrolase/aminopeptidase, the gatekeeper of chemotactic leukotriene B4 biosynthesis. *J. Biol. Chem.* **2004**, *279*, 50639−42.

(41) Thoren, S.; Weinander, R.; Saha, S.; Jegerschold, C.; Pettersson, P. L.; Samuelsson, B.; Hebert, H.; Hamberg, M.; Morgenstern, R.; Jakobsson, P. J. Human microsomal prostaglandin E synthase-1 - Purification, functional characterization, and projection structure determination. *J. Biol. Chem.* **2003**, *278*, 22199−22209.

(42) Kulmacz, R. J.; Lands, W. E. M. Requirements for Hydro-peroxide by the Cyclooxygenase and Peroxidase-Activities of Prostaglandin-H Synthase. *Prostaglandins* **1983**, *25*, 531−540.

(43) Jiang, X. L.; Zhou, L.; Wei, D. G.; Meng, H.; Liu, Y.; Lai, L. H. Activation and inhibition of leukotriene A(4) hydrolase amino-peptidase activity by diphenyl ether and derivatives. *Bioorg. Med. Chem. Lett.* **2008**, *18*, 6549−6552.

(44) Wang, Q.; Qi, Y. F.; Yin, N.; Lai, L. H. Discovery of Novel Allosteric Effectors Based on the Predicted Allosteric Sites for Escherichia coli D-3-Phosphoglycerate Dehydrogenase. *PLoS One* **2014**, *9*, 9.